Title

Parallel responses of human epidermal keratinocytes to inorganic SbIII and AsIII

Journal

Environmental Chemistry, 13(6)

ISSN

1448-2517

Authors

Phillips, Marjorie A

Cánovas, Angela

Wu, Pei-Wen

et al.

Publication Date

2016

DOI

10.1071/en16019

Peer reviewed

HHS Public Access

Author manuscript

Environ Chem. Author manuscript; available in PMC 2017 July 12.

Published in final edited form as:

Environ Chem. 2016 ; 13(6): 963–970. doi:10.1071/EN16019.

Parallel responses of human epidermal keratinocytes to inorganic SbIII and AsIII

Marjorie A. Phillips[A], **Angela Cánovas**[B,C], **Pei-Wen Wu**[A], **Alma Islas-Trejo**[B], **Juan F. Medrano**[B], and **Robert H. Rice**[A,*]

[A]Department of Environmental Toxicology, University of California, Davis, CA 95616

[B]Department of Animal Science, University of California, Davis, CA 95616

Abstract

SbIII and AsIII are known to exhibit similar chemical properties, but the degree of similarity in their effects on biological systems merits further exploration. Present work compares the responses of human epidermal keratinocytes, a known target cell type for arsenite-induced carcinogenicity, to these metalloids after treatment for a week at environmentally relevant concentrations. Previous work with these cells has shown that arsenite and antimonite have parallel effects in suppressing differentiation, altering levels of several critical enzymes and maintaining colony forming ability. More globally, protein profiling now reveals parallels in SbIII and AsIII effects. The more sensitive technique of transcriptional profiling also shows considerable parallels. Thus, gene expression changes were almost entirely in the same directions for the two treatments, although the degree of change was sometimes significantly different. Inspection of the changes revealed that RYR1 and LRIG1 were among the genes strongly suppressed, consistent with reduced calcium-dependent differentiation and maintenance of EGF-dependent proliferative potential. Moreover, levels of miRNAs in the cells were altered in parallel, with nearly 90% of the 198 most highly expressed ones being suppressed. Among these was miR-203, which is known to decrease proliferative potential. Finally, both SbIII and AsIII were seen to attenuate bone morphogenetic protein 6 induction of dual specificity phosphatases 2 and 14, consistent with maintaining epidermal growth factor receptor signaling. These findings raise the question whether SbIII, like AsIII, could act as a human skin carcinogen.

Introduction

Use of antimony in commerce is at a high level and increasing, to which increasing atmospheric contamination attests.[1] Mining and smelting operations for this metalloid around the world have resulted in high local levels in soils[2] and remarkably high bioaccumulation in some aquatic species in affected watersheds.[3] Disposal and recycling of waste electrical and electronic equipment has been noted to result in local high environmental contamination at least in part due to plastics containing antimony as a catalyst or flame retardant. Problems with antimony contamination have become especially

*Corresponding author. rhrice@ucdavis.edu.

[C]Current affiliation: University of Guelph, Centre for Genetic Improvement of Livestock, Department of Animal Bioscience, Guelph, ON N1G 2W1, Canada

conspicuous in China,[4] where levels in fish near a mining area[5] and even household dust due to recycling operations[6] can be considerably elevated.

Increasing antimony exposure due to environmental accumulation has raised concerns about possible health effects for humans and ecosystems. The similarity of AsIII and SbIII in biological actions can be rationalized by their known similarity in chemical properties. Immediately beneath As in the periodic table, Sb has a similar outer electron orbital configuration. This similarity leads to the same basic crystal structures for AsIII and SbIII oxides. However, crystals of AsV and SbV oxides pack quite differently due to the slightly larger size of the latter. This distinction in size and geometry,[7, 8] which can affect interactions with macromolecules,[9] may help rationalize that SbV has little obvious biological activity in human keratinocytes, indicating the rate of reduction to SbIII in them is too low to produce effects, despite the facile AsV reduction to AsIII in this cell type.[10]

Comparison of the actions of arsenite (AsIII) and antimonite (SbIII) has revealed considerable parallels in responses of cultured human epidermal cells, a well-known arsenic target cell type, where antimonite displayed nearly half the potency of arsenite. SbIII accumulates in cultured keratinocytes to approximately half the concentration of AsIII, and with similar kinetics, when administered at the same concentration in the medium.[10] Keratinocytes respond similarly to SbIII and AsIII in perturbation of normal function. [10–13] Both suppress differentiation markers (keratins, cell size). They prolong epidermal growth factor receptor (EGFR) pathway signaling as judged by maintaining colony forming ability at confluence and preventing suppression of EGFR signaling by insulin. Also, they alter levels of critical enzymes, including protein kinase C delta (PKCδ), notch intracellular domain (NICD), and matrix metalloproteinase 7 (MMP7). The result is to suppress differentiation and to maintain the proliferative state. Observation of these similarities and differences raises the question whether Sb, like As, can act as a human skin carcinogen.

Experimental

Cell culture

Spontaneously immortalized human epidermal keratinocytes (SIK) were cultured with 3T3 feeder layer support in a 2:1 mixture of Dulbecco-Vogt Eagle’s and F12 media supplemented with fetal bovine serum (5%), epidermal growth factor (10 ng/ml), hydrocortisone (0.4 μg/ml), insulin (5 μg/ml), transferrin (5 μg/ml) and adenine (0.18 mM). [10–13] The cultures were treated with 3 μM sodium arsenite or 6 μM potassium antimony tartrate starting at confluence and harvested 7 days later. Previous work has shown that SbIII accumulates in keratinocytes to approximately half the concentration of AsIII with similar kinetics when administered at the same concentration in culture medium.[10] The arsenite and antimonite reagents employed were determined by ICP mass spectrometry to have negligible contamination by antimony and arsenic, respectively.[10]

Proteomic sample preparation

Treated cultures were rinsed twice in phosphate buffered saline, scraped into microfuge tubes and stored frozen until processing. The protein was reduced in 2% sodium

dodecanoate – 25 mM dithioerythritol – 50 mM ammonium bicarbonate and alkylated with 50 mM iodoacetamide, extracted twice with ethyl acetate after acidification with 0.1% trifluoroacetate, readjusted to pH 8 with ammonia and ammonium bicarbonate, digested with reductively methylated trypsin,[14] clarified by centrifugation and submitted for mass spectrometric analysis. Four experiments, where cultures were either not treated or treated with antimonite or arsenite, were analyzed.

Protein identification

Digested peptides were analyzed by LC-MS/MS with a Thermo Scientific Q Exactive Plus Orbitrap mass spectrometer essentially as previously described.[15] Sample data were analyzed using X!Tandem (Cyclone 2013.02.01.1) to search a Uniprot human database appended to a database of common non-human contaminants (cRAP, common Repository of Adventitious Proteins database, http://www.thegpm.org/crap/). Both were appended to an identical but reversed database for estimating false discovery rates (137,120 entries total), assuming the digestion enzyme was trypsin. X!Tandem was searched with a fragment ion mass tolerance of 20 ppm and a parent ion tolerance of 20 ppm. Iodoacetamide derivative of cysteine was specified in X!Tandem as a fixed modification. Glu/Gln- > pyro-Glu (N-term), deamidation of asparagine and glutamine, oxidation of methionine and tryptophan, dioxidation of methionine and tryptophan, N-terminal acetylation, and ammonia loss were specified in X!Tandem as variable modifications. Scaffold version 4.4.3 was used to validate MS/MS based peptide and protein identifications. Peptide identifications were accepted if they could be established at greater than 99% probability as specified by the Peptide Prophet algorithm (peptide decoy false discovery rate 0.0%). Protein identifications were accepted if they contained at least two identified peptides (protein decoy false discovery rate 0.2%). Protein probabilities were assigned by the Protein Prophet algorithm. Since certain peptides can overlap among the keratins, data were analyzed in parallel by exclusive spectral counts to ensure the weighted spectral counts (presented) were genuine. The statistical analysis (t-testing) was performed on normalized and transformed weighted spectral counts as for the transcriptomic data. Responses that differed with $p < 0.05$ and a fold change > 2 were analyzed further. In comparing direction of change for a significantly changed protein, the corresponding value in the full set of 824 proteins was used. An Excel file of these proteins and their spectral counts is available at http://etox.ucdavis.edu/directory/faculty/rice-robert/.

miRNA analysis

Total RNA was prepared using a mirVANA miRNA isolation kit from Ambion designed to result in good yields of small RNAs. Samples were analyzed without enriching for the small RNA fraction. miRNA profiling was performed using miRNA Megaplex RT, preamplification reagents and arrays (v2, A and B pools) from Applied Biosystems. Array results were analyzed with Applied Biosystems software and normalized to MAMMU6 expression levels. Differential expression due to arsenic and antimony treatment was determined by comparison to levels of miRNAs in untreated cultures. Individual miRNA expression levels were confirmed by qPCR using Taqman miRNA assays (Applied Biosystems).

miRNA overexpression

Overexpression of miRNAs was achieved using lentiviral miRNA precursor constructs from System Biosciences. Viral particles were prepared in HEK293 cells by co-transfection of the miRNA precursor constructs with packaging plasmids from Life Technologies. Pre-confluent keratinocyte cultures were transduced with viral particles in 6 well plates. Transduction efficiency was monitored by fluorescence microscopy of co-expressed GFP, which showed that a majority of the cells were transduced. In some experiments cells over-expressing miRNAs were treated with sodium arsenite or potassium antimony tartrate at confluence for 7 days, then harvested for differentiation marker expression by qPCR or colony forming efficiency (a measure of proliferative potential), as previously described.[11] Analysis focused on the most prevalent miRNAs, those with control values ≤30 for CT, the cycle at which the product concentration threshold was reached.

Transcriptomic analysis

Total mRNA was prepared using Trizol reagent from two independent experiments. Sequencing libraries were prepared using an Illumina TrueSeq mRNA Sample Preparation kit. mRNA was purified and converted to double stranded cDNA. Adapters and specific indexes were added to each sample. RNA sequencing was performed on a HiSeq 2500 sequencer analyzer (Illumina, San Diego, CA). Sequencing reads were analyzed using CLCBio Genomic workbench software (CLC Bio, Aarhus, Denmark).[16] Quality control (QC) analysis was performed using the application NGS quality control tool of CLC Genomics workbench software (CLC Bio, Aarhus, Denmark).[17] This tool assesses sequence quality indicators based on the FastQC-project (http://www.bioinformatics.babraham.ac.uk/projects/fastqc/). Quality was measured taking into account sequence-read lengths and base-coverage, nucleotide contributions and base ambiguities, quality scores as emitted by the base caller and over-represented sequences. The samples analyzed passed all the QC parameters having the same length (100bp), 100% coverage in all bases, 25% of A, T, G and C nucleotide contributions, 50% GC base content and less than 0.1% over-represented sequences, indicating very good quality.[18] Sequenced single reads (100 bp) were assembled against the annotated human reference genome (release 80) (ftp://ftp.ensembl.org/pub/release-80/genbank/homo_sapiens/). Data were normalized by calculating the ‘reads per kilobase per million mapped reads’ (RPKM) for each gene.[18] To select expressed genes a threshold of RPKM ≥ 0.2 was used,[19] providing ≈15,000 genes. Normalization and transformation of the data were performed to change the expression data from negative binomial to normal distribution. Differential expression analysis between control and treated (arsenic or antimony) human epidermal keratinocytes cells was performed by t-test. An Excel file of the sequencing results is available at http://etox.ucdavis.edu/directory/faculty/rice-robert/.

qPCR

RNA was harvested from cells treated for 1 week with 50 ng/ml BMP in the presence or absence of arsenite or antimonite. RNA was prepared using Trizol, transcribed to cDNA using an Applied Biosystems cDNA reverse transcription kit and analyzed by qPCR with Taqman assays. Results were normalized to GusB housekeeping gene expression.

Results

Shotgun protein profiling was performed using mass spectrometry of tryptic peptides obtained from whole cell extracts of untreated cells or cells treated with 3 μM sodium arsenite or 6 μM potassium antimony tartrate. As shown in Fig 1, of the 824 proteins reproducibly detected, antimonite suppressed levels of 25 and stimulated levels of 24. Similarly, arsenite suppressed levels of 33 proteins and stimulated levels of 18. When the responses to the two treatments were compared, considerable overlap was evident in that 17 proteins were suppressed by both, and 10 were stimulated by both. Of the 41 total proteins suppressed by one treatment, only 3 were stimulated by the other treatment. Of the 32 proteins stimulated by one treatment, none were suppressed by the other. Thus, the differences in the two treatments were primarily the degree of change rather than its direction. When the levels of proteins in the two treatments were compared directly, 14 of the 824 detected proteins were judged significantly different. Eight were significantly higher and 6 lower in the antimonite treated cultures than in the arsenite treated cultures. Among these 14, as shown in Fig. 2, 10 differed significantly from untreated in the same direction, while 4 displayed changes in different directions.

Results of the more sensitive next generation sequencing also indicate that inorganic AsIII and SbIII produced highly similar transcriptional responses in human keratinocytes. As previously observed by DNA microarray for arsenite,[20] more genes were suppressed than stimulated by the treatments. A total of 430 genes were seen to be differentially expressed at a high level of statistical stringency ($p < 0.01$). Of those with fold change > 2, 96 had higher levels in the antimonite treated cultures, and 36 had higher levels in the arsenite treated cultures (Fig 3). Although the levels of these 132 mRNAs were significantly different, they were nearly all changed in the same direction (stimulated or suppressed by both) compared to the untreated cultures. Of those suppressed by arsenite, only one was stimulated by antimonite, and of those stimulated by antimonite, only two were suppressed by arsenite. At a stringency level of $p < 0.05$, 1202 genes were suppressed and 582 were stimulated in common by antimonite and arsenite with 2% that number regulated in opposite directions. Particularly striking were parallel changes in differentiation marker expression, metabolic enzymes and proteins regulated by the Nrf2 signaling pathway (Table 1). Among the newly discovered mRNAs down-regulated by arsenite and antimonite are those encoding LRIG1, a negative regulator of EGFR signaling, and ryanodine receptor 1 (RYR1), a positive regulator of calcium signaling that promotes cell differentiation (Fig. 4).

Since miRNAs have important regulatory roles in cells, alterations in miRNA expression levels were determined using real time PCR arrays. Among the 198 most highly expressed miRNAs, 134 were unchanged in cultures treated with arsenite or antimonite, 56 were decreased and 6 were increased; only two miRNAs were differentially regulated (Fig. 5). Several of the miRNAs found to be decreased by arsenite and antimonite treatments were verified by single real time PCR Taqman assays, including miR-143, miR-146a (not shown) and miR-203 (Fig 6A). To investigate a potential link between suppression of mi-RNAs and differentiation markers, miR-143, miR-146a and miR-203 were separately over-expressed in cultured keratinocytes, resulting in a 4-fold increase for miR-203, 100-fold for miR-143 and 400-fold for miR-146a. While the latter two mi-RNAs appeared to accelerate cell growth,

miR-203 over-expression was growth inhibitory, which may explain the relatively modest levels of miR-203 over-expression achieved. None of these miRNAs had much effect on expression of differentiation markers or on the ability of arsenite or antimonite to suppress their expression (not shown). Since arsenite and antimonite preserve proliferative potential while miR-203 expression results in its loss, we investigated whether the decrease in miR-203 levels by arsenite and antimonite could contribute to this phenomenon. Over-expression of miR-203 resulted in the expected loss in colony forming efficiency while arsenite and antimonite increased it. Over-expression of miR-203 was able to attenuate the increased colony forming efficiency elicited by arsenite and antimonite (Fig. 6B).

The high correspondence of responses due to arsenite and antimonite treatment resulting in altered protein, mRNA and miRNA levels suggests that common cell signaling pathways are targeted by these metalloids. Previous work has demonstrated similar changes in EGFR and Notch signaling.[11, 12] We have now shown that bone morphogenetic protein (BMP6) induction of DUSP2 and DUSP14 is attenuated by antimonite (Fig. 7) as well as arsenite treatment.[21] Key signaling pathways affected by both agents are summarized in Fig. 8. In general, arsenite and antimonite prolong EGFR signaling and proliferative potential, perhaps by induction of LRIG1, while they suppress pro-differentiation pathways such as NOTCH1 and BMP6.

Discussion

Previous work has indicated that AsIII and SbIII produce similar effects in human keratinocytes. Their parallel effects on major signaling pathways result overall in suppressing differentiation and preserving proliferative potential. Present work gives a more comprehensive accounting of their degree of similarity, demonstrating parallels in transcript, protein and miRNA levels. They both induce enzymes of anaerobic fermentation, previously noted for arsenite,[22] and NRF2-dependent signaling while suppressing numerous differentiation markers. The results also reveal further parallels not previously known. For example, their suppression of LRIG1, which attenuates EGFR signaling, and RYR1, which helps regulate cytoplasmic calcium levels and thus differentiation, provide further rationale for the profoundly parallel effects these agents have. Further analysis of the differential expression may help reveal whether they have significant differences in their biological effects.

Antimony (diantimony trioxide) is classified as a carcinogen based on its induction of lung cancer in female rats from high level inhalation exposure. However, the magnitude of the exposure level raises the possibility that an overload of poorly soluble particles induced an inflammatory response yielding fibrosis and tumors, an effect of a threshold carcinogen.[23, 24] While this interpretation may minimize the carcinogenic risk of human exposure, the difficulty in demonstrating animal carcinogenicity of arsenic must be kept in mind. Though long established in humans, it was not clearly shown to be carcinogenic in animals until the results of transplacental exposure became available.[25] Moreover, arsenic co-carcinogenicity for the skin with UV light has also been demonstrated.[26] Difficulties in showing carcinogenicity in animals reflects at least in part the much greater sensitivity of humans. In view of the parallels in SbIII and AsIII action in keratinocytes, particularly those

maintaining growth capability, animal testing of diantimony trioxide in the same ways would be prudent. Moreover, while some impairment of nucleotide excision repair has been reported by antimony,[27] testing possible impairment of PARP1 would also be useful, inasmuch as this phenomenon helps explain the co-mutagenicity/carcinogenicity of arsenite with UV light.[28] Extension to antimonite of the reported sensitivity of zinc finger proteins to oxidation by trivalent arsenic[29] could help explain the observed parallels in transcriptional response.

While the trivalent forms of antimony and arsenic produce nearly parallel effects and thus could plausibly be similarly carcinogenic, the outcome of SbV exposure is more uncertain. While SbV can be reduced nonenzymatically to SbIII by glutathione at low pH,[30] its inactivity in cultured human keratinocytes probably reflects a lack of reduction at neutral pH. Reduction in vivo does take place in individuals treated for leishmaniasis[31] and is seen in macrophages[32] and blood[33], presumably occurs in the stomach and may occur at other sites. In keratinocytes, SbIII is nearly half as potent as AsIII, but SbV is much less potent than AsV since the latter is readily converted to AsIII in cells. Thus the risk attributable to SbV depends not only on the level of direct exposure but also on its rate of reduction, likely tissue (and species) dependent. The possibility that SbV has biological activity in tissue targets beyond the epidermis cannot be excluded.

Acknowledgments

We thank Dr. Brett Phinney and Michelle Salemi (Proteomics Core Facility) for expert proteomic assistance, Tammi Olineka (Real-time PCR Research and Diagnostic Core Facility) for assistance with miRNA arrays, Drs. Kirk Nordstrom and Waldo Quiroz for valuable suggestions and the Qb3 Vincent J. Coates Genomics Sequencing Laboratory at the University of California, Berkeley for RNA sequencing. This work was supported in part by NIH grant P42 ES04699.

References

1. Krachler M, Zheng J, Koerner R, Zdanowicz C, Fisher D, Shotyk W. Increasing atmospheric antimony contamination in the northern hemisphere: snow and ice evidence from Devon Island, Arctic Canada. J Environ Monit. 2005; 7:1169–76. [PubMed: 16307068]
2. Wilson SC, Lockwood PV, Ashley PM, Tighe M. The chemistry and behaviour of antimony in the soil environment with comparisons to arsenic: a critical review. Environ Pollut. 2010; 158:1169–81. [PubMed: 19914753]
3. Dovick MA, Kulp TR, Arkle RS, Pilliod DS. Bioaccumulation trends of arsenic and antimony in a freshwater ecosystem affected by mine drainage. Environmental Chemistry. 2016; 13:149–59.
4. He M, Wang X, Wu F, Fu Z. Antimony pollution in China. Sci Total Environ. 2012; 421–422:41–50.
5. Fu Z, Wu F, Amarasiriwardena D, Mo C, Liu B, Zhu J, et al. Antimony, arsenic and mercury in the aquatic environment and fish in a large antimony mining area in Hunan, China. Sci Total Environ. 2010; 408:3403–10. [PubMed: 20452645]
6. Bi X, Li Z, Zhuang X, Han Z, Yang W. High levels of antimony in dust from e-waste recycling in southeastern China. Sci Total Environ. 2011; 409:5126–8. [PubMed: 21907394]
7. Pauling L. The formulas of antimonic acid and the antimonates. Proc Natl Acad Sci USA. 1933; 55:1895–900.
8. Allen JP, Carey JJ, Walsh A, Scanlon DO, Watson GW. Electronic structures of antimony oxides. J Phys Chem C. 2013; 117:14759–69.
9. Campbell KM, Nordstrom DK. Arsenic speciation and sorption in natural environments. Rev Mineral Geochem. 2014; 79:185–216.

10. Patterson TJ, Ngo M, Aronov PA, Reznikova TV, Green PG, Rice RH. Biological activity of inorganic arsenic and antimony reflects oxidation state in cultured keratinocytes. Chem Res Toxicol. 2003; 16:1624–31. [PubMed: 14680377]
11. Patterson TJ, Rice RH. Arsenite and insulin exhibit opposing effects on epidermal growth factor receptor and keratinocyte proliferative potential. Toxicol Appl Pharmacol. 2007; 221:119–28. [PubMed: 17400267]
12. Reznikova TV, Phillips MA, Rice RH. Arsenite suppresses Notch1 signaling in human keratinocytes. J Invest Dermatol. 2009; 129:155–61. [PubMed: 18633435]
13. Reznikova TV, Phillips MA, Patterson TJ, Rice RH. Opposing actions of insulin and arsenite converge on PKCδ to alter keratinocyte proliferative potential and differentiation. Molec Carcinogen. 2010; 49:398–409.
14. Rice RH, Means GE, Brown WD. Stabilization of bovine trypsin by reductive methylation. Biochim Biophys Acta. 1977; 492:316–21. [PubMed: 560214]
15. Kumar V, Bouameur J-E, Bär J, Rice RH, Hornig-Do H-T, Roop DR, et al. A keratin scaffold regulates epidermal barrier formation, mitochondrial lipid composition and activity. J Cell Biol. 2015; 211:1057–75. [PubMed: 26644517]
16. Wickramasinghe S, Cánovas A, Rincón G, Medrano JF. RNA-sequencing: a tool to explore new frontiers in animal genetics. Livestock Science. 2014; 166:206–16.
17. Cánovas A, Rincón G, Islas-Trejo A, Jimenez-Flores R, Laubscher A, Medrano JF. RNA sequencing to study gene expression and single nucleotide polymorphism variation associated with citrate content in cow milk. J Dairy Sci. 2013; 96:2637–48. [PubMed: 23403202]
18. Cánovas A, Rincón G, Bevilacqua C, Islas-Trejo A, Brenaut P, Hovey RC, et al. Comparison of five different RNA sources to examine the lactating bovine mammary gland transcriptome using RNA-Sequencing. Scientific Reports. 2014; 4:5297. [PubMed: 25001089]
19. Wickramasinghe S, Rincon G, Islas-Trejo A, Medrano JF. Transcriptional profiling of bovine milk using RNA sequencing. BMC Genomics. 2012; 13:45. [PubMed: 22276848]
20. Rea MA, Gregg JP, Qin Q, Phillips MA, Rice RH. Global alteration of gene expression in human keratinocytes by inorganic arsenic. Carcinogenesis. 2003; 24:747–56. [PubMed: 12727804]
21. Phillips MA, Qin Q, Hu Q, Zhao B, Rice RH. Arsenite suppression of BMP signaling in human keratinocytes. Toxicol Appl Pharmacol. 2013; 269:290–6. [PubMed: 23566955]
22. Lee C, Lee YM, Rice RH. Human epidermal cell protein responses to arsenite treatment in culture. Chem-Biol Interact. 2005; 155:43–54. [PubMed: 15899475]
23. Swedish Chemicals Inspectorate, Diantimony Trioxide Risk Assessment, Sundbyberg, Sweden. 2008. Available from: https://www.google.com/search?q=European+Union+Risk+Assessment+Report+DIANTIMONY+TRIOXIDE&ie=utf-8&oe=utf-8
24. EPA Assessment Team. TSCA Work Plan Chemical Risk Assessment Antimony Trioxide. 2014.
25. Waalkes MP, Liu J, Diwan BA. Transplacental arsenic carcinogenesis in mice. Toxicol Appl Pharmacol. 2007; 222:271–80. [PubMed: 17306315]
26. Rossman TG, Uddin AN, Burns FJ. Evidence that arsenite acts as a cocarcinogen in skin cancer. Toxicol Appl Pharmacol. 2004; 198:394–404. [PubMed: 15276419]
27. Grosskopf C, Schwerdtle T, Mullenders L, Hartwig A. Antimony impairs nucleotide excision repair: XPA and XPE as potential molecular targets. Chem Res Toxicol. 2010; 23:1175–83. [PubMed: 20509621]
28. Zhou X, Sun X, Cooper KL, Wang F, Liu KJ, Hudson LG. Arsenite interacts selectively with zinc finger proteins containing C3H1 or C4 motifs. J Biol Chem. 2011; 286:22855–63. [PubMed: 21550982]
29. Zhou X, Cooper KL, Sun X, Liu KJ, Hudson LG. Selective sensitization of zinc finger protein oxidation by reactive oxygen species through arsenic binding. J Biol Chem. 2015; 290:18361–9. [PubMed: 26063799]
30. Frézard F, Demicheli C, Ferreira CS, Costa MA. Glutathione-induced conversion of pentavalent antimony to trivalent antimony in meglumine antimoniate. Antimicrob Agents Chemother. 2001; 45:913–6. [PubMed: 11181379]

31. Miekeley N, Mortari SR, Schubach AO. Monitoring of total antimony and its species by ICP-MS and on-line ion chromatography in biological samples from patients treated for leishmaniasis. Anal Bioanal Chem. 2002; 372:495–502. [PubMed: 11939540]

32. Hansen C, Hansen EW, Hansen HR, Gammelgaard B, Stürup S. Reduction of Sb(V) in a human macrophage cell line measured by HPLC-ICP-MS. Biol Trace Elem Res. 2011; 144:234–43. [PubMed: 21618006]

33. López S, Aguilar L, Mercado L, Bravo M, Quiroz W. Sb(V) reactivity with human blood components: redox effects. PLoS One. 2015; 10(1):e0114796. [PubMed: 25615452]

Environmental context

Increasing commercial use of antimony is raising its environmental presence and thus possible effects on humans and ecosystems. An important uncertainty is the risk that exposure poses for biological systems. The present work explores the similarity in response of human epidermal keratinocytes, a known target cell type, to SbIII and AsIII, where deleterious consequences of exposure to the latter are better known.

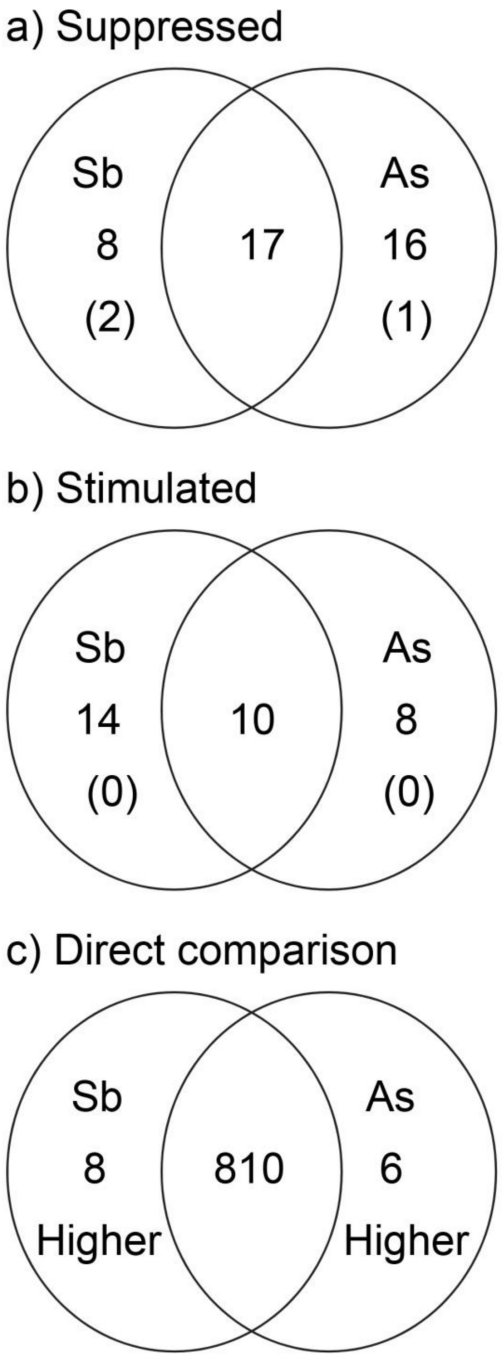

Fig 1.

Significant differences in protein level ($p < 0.05$ and fold change >2). (a) Shown is the distribution of the 41 suppressed proteins, where those in parentheses are the number regulated in the opposite direction by the other treatment. (b) The distribution of stimulated proteins is shown, where none were regulated in the opposite direction. (c) The distribution of the 14 significantly different protein levels between cultures treated with SbIII or AsIII.

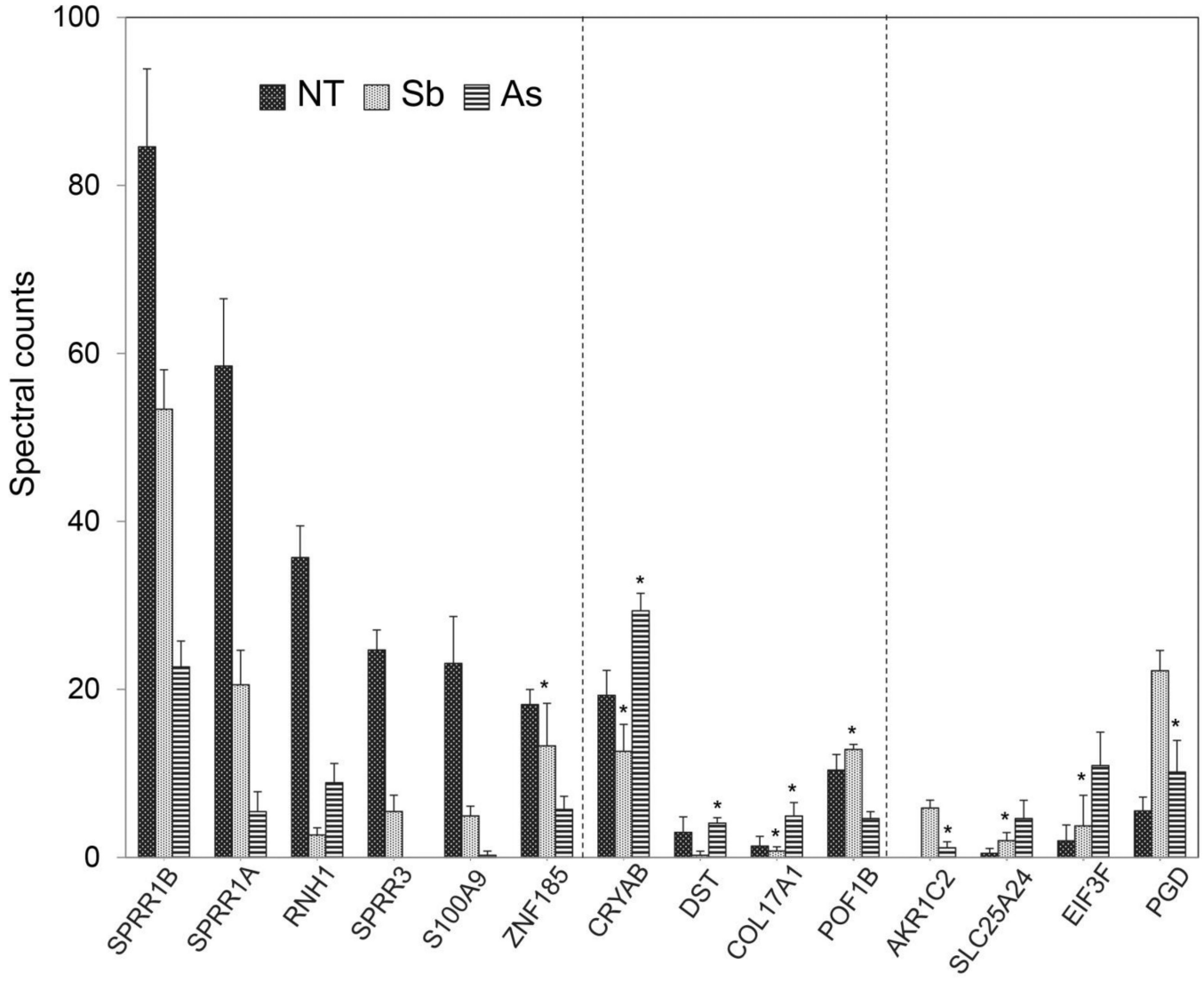

Fig 2.

Peptide spectral counts of the 14 proteins showing significantly different levels in cultures treated with SbIII or AsIII. The 6 proteins at left were suppressed by both agents compared to untreated cultures, the 4 proteins on the right were stimulated by both agents, and the 4 in the middle were changed in opposite directions. The values in treated cultures were all significantly different from those in untreated (NT) cultures except for those indicated by asterisks (*).

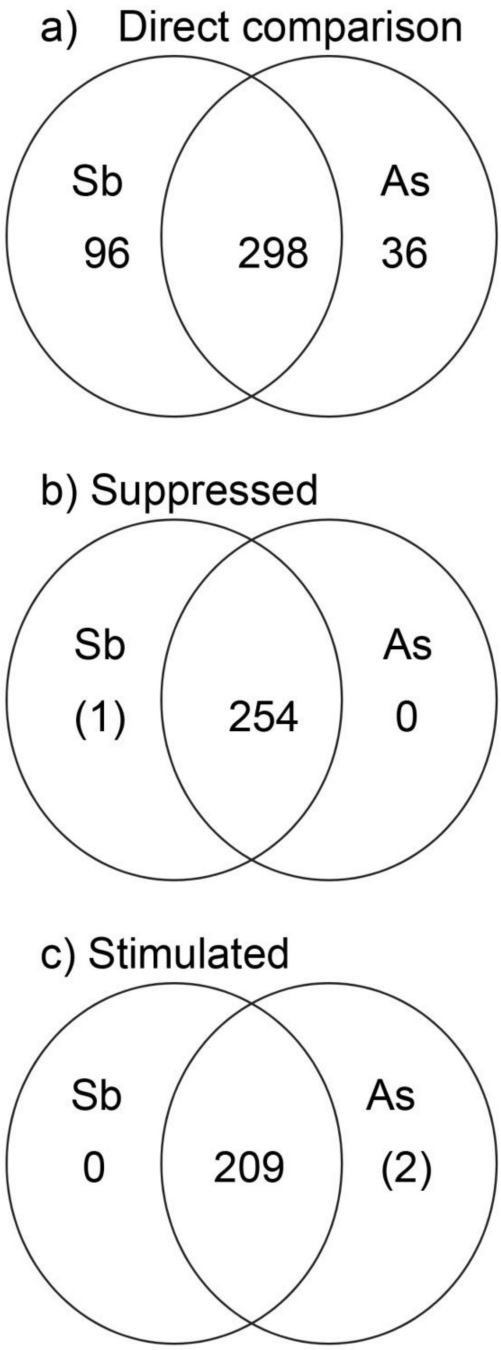

Fig 3.

Differentially expressed genes resulting from treatment with SbIII or AsIII. (a) Of the 430 genes differentially expressed ($p \leq 0.01$ and fold change ≥ 2), 96 were higher in SbIII treated and 36 were higher in AsIII treated cultures. Also shown are the distributions of genes either suppressed (b) or stimulated (c), where numbers in parentheses show those expressed in opposite directions with the other treatment.

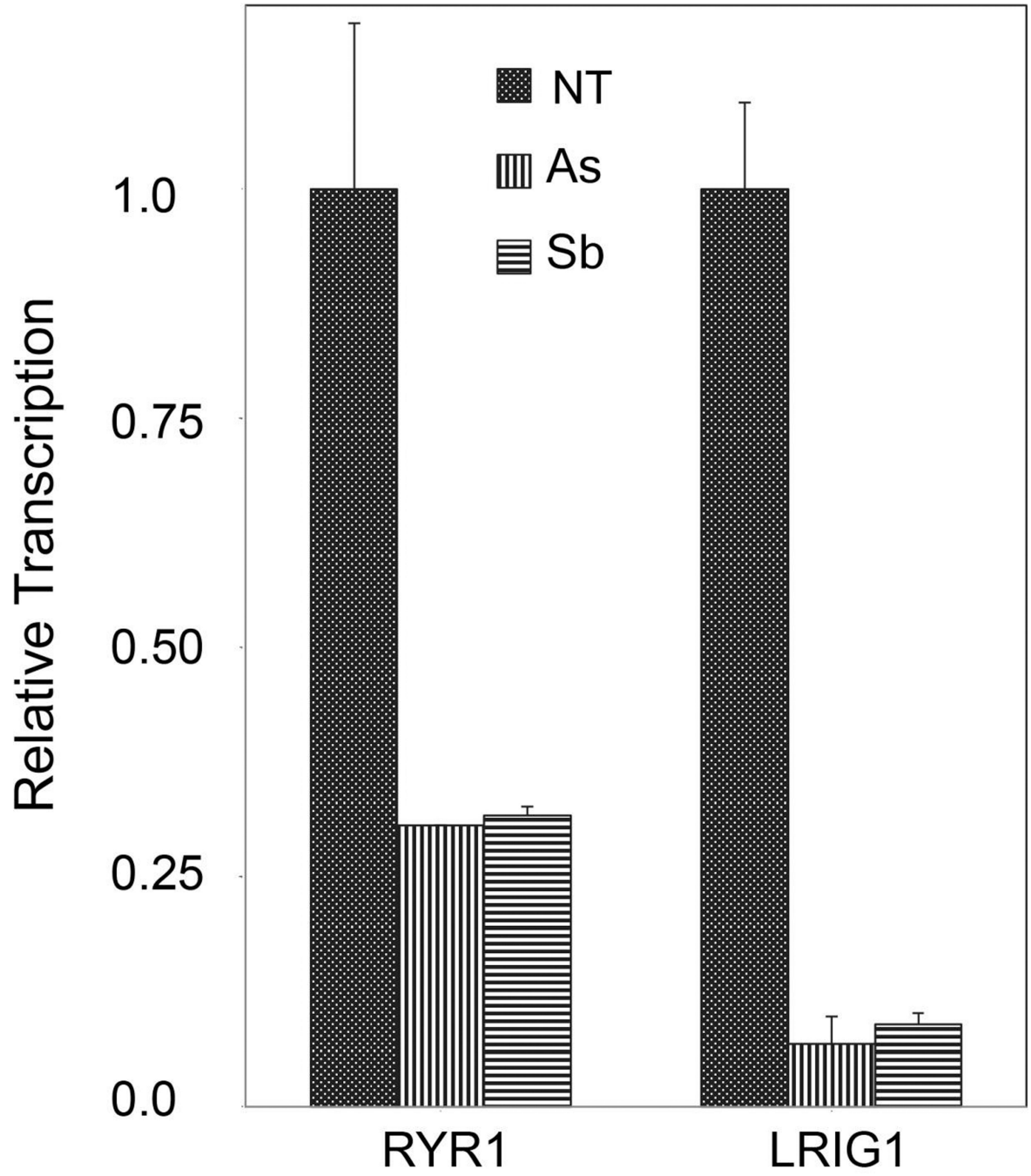

Fig 4.

Suppression of RYR1 and LRIG1 transcription by SbIII and AsIII. Normalization to levels in untreated cultures (RPKM values of 1.2 and 0.4, respectively) showed at least 3 fold suppression for RYR1 and 10 fold for LRIG1. NT, not treated.

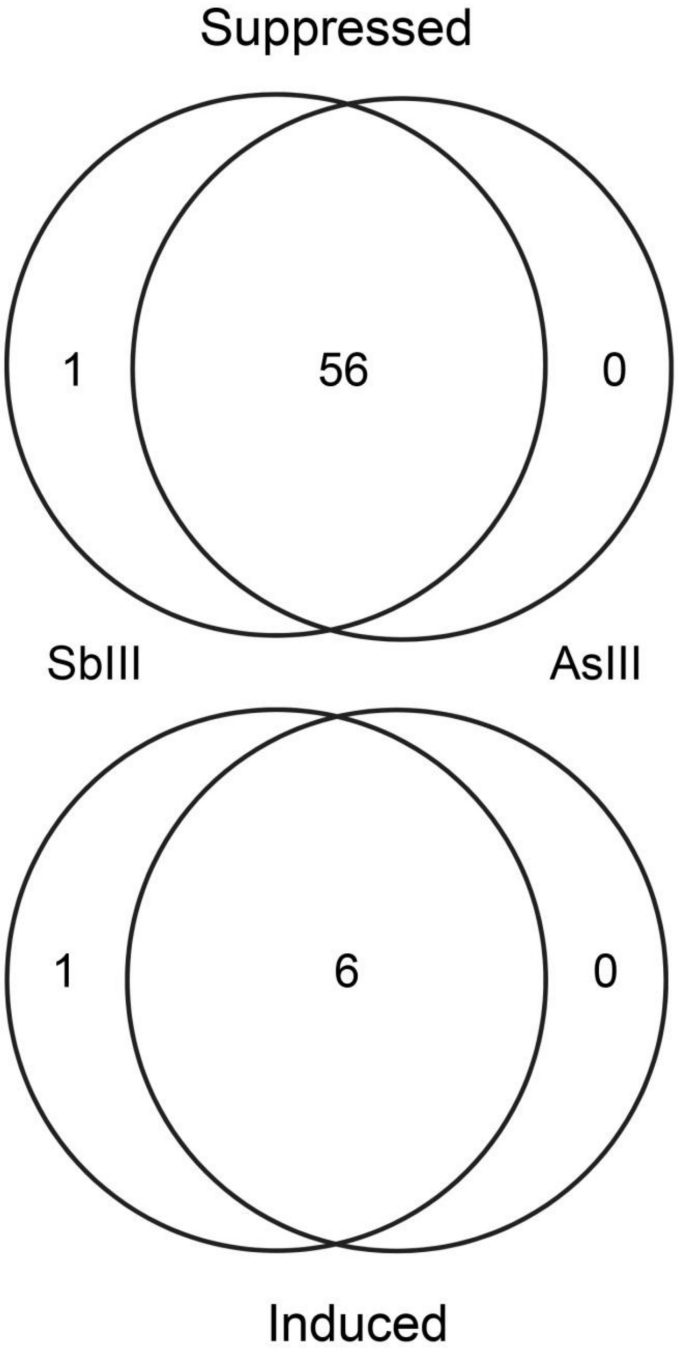

Fig 5.

Venn diagram of differentially expressed miRNAs resulting from treatment with SbIII or AsIII. miRNAs were classified as decreased if amounts were ≤0.5 compared to the untreated control and were classified as increased if amounts were ≥1.5 compared to control. miRNAs were reported as regulated differently with AsIII and SbIII if they were increased by one agent and decreased by the other.

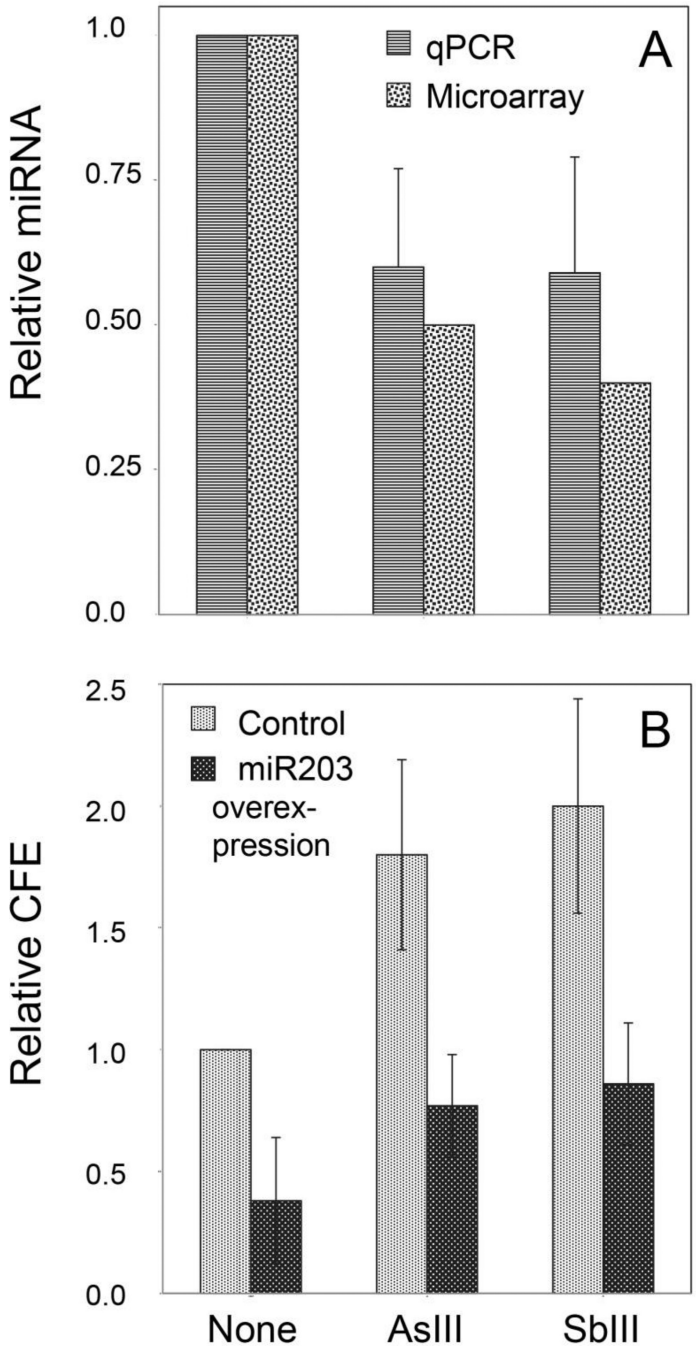

Fig 6.

Effects of SbIII and AsIII on miR203 expression and proliferative potential. (a) miR203 levels were measured by array or qPCR. Results of qPCR were the mean and standard deviation of 6 independent experiments. miR203 levels were significantly different from the no treatment control at $p \leq 0.005$ determined by t-test. (b) Proliferative potential was measured by colony forming efficiency assays on cultures over-expressing miR203 or empty vector after 1 week of treatment. Results of 3 independent experiments are normalized to the

untreated cultures not over-expressing mi203, which is set as 1. Significant differences due to miR203 over-expression ($p \leq 0.01$) were determined by t-test.

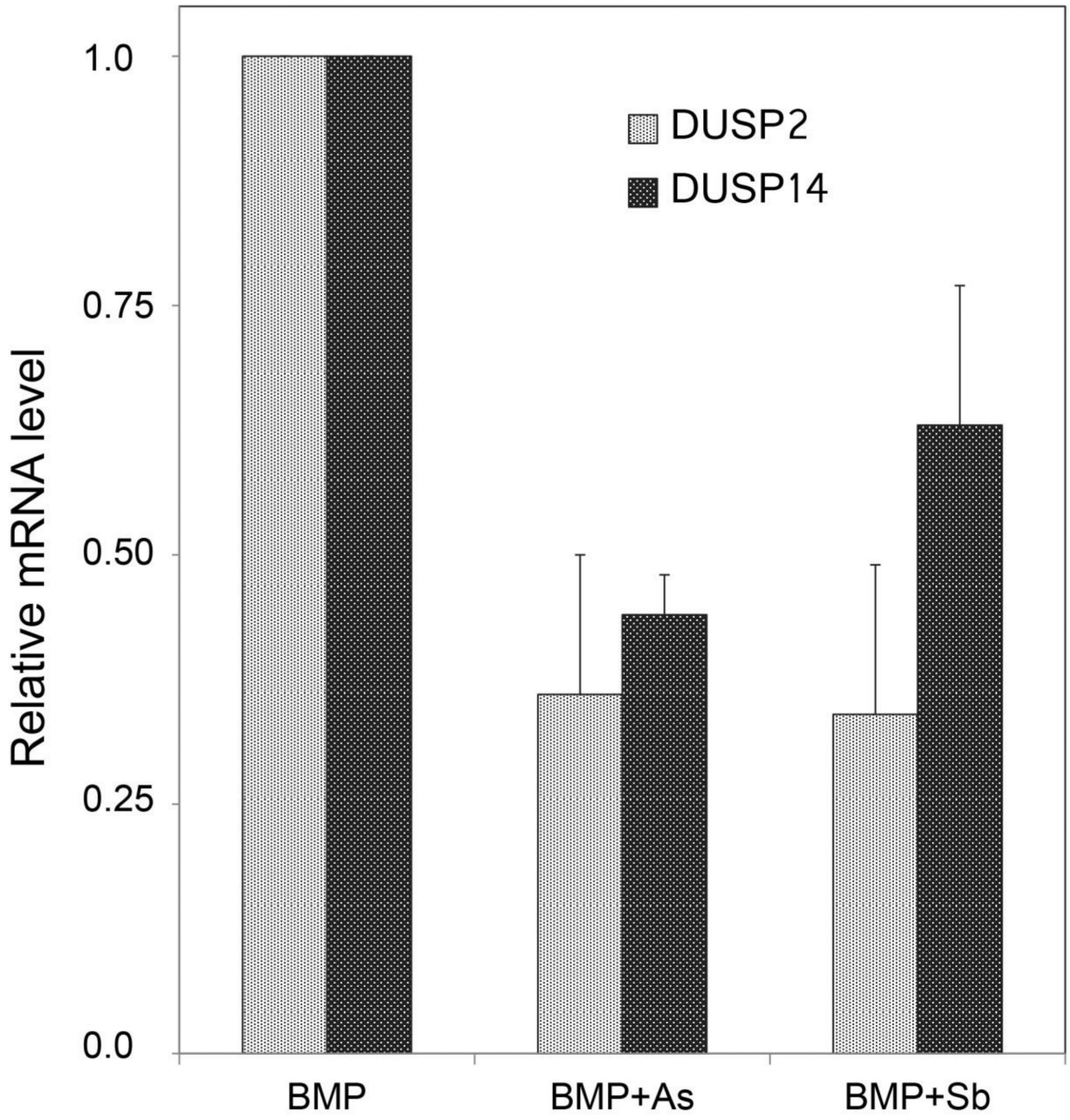

Fig 7.

Attenuation of BMP6 induction of DUSP2 and DUSP14 by treatment with SbIII or AsIII. DUSP mRNA levels were determined by qPCR and normalized to amounts in samples treated with BMP6 only, set at 1. Results are shown as the mean and standard deviation of 4 experiments. DUSP mRNA levels after treatment with arsenic + BMP6 and antimony + BMP6 were significantly different from BMP alone at $p < 0.01$ as determined by t-test with Bonferroni correction.

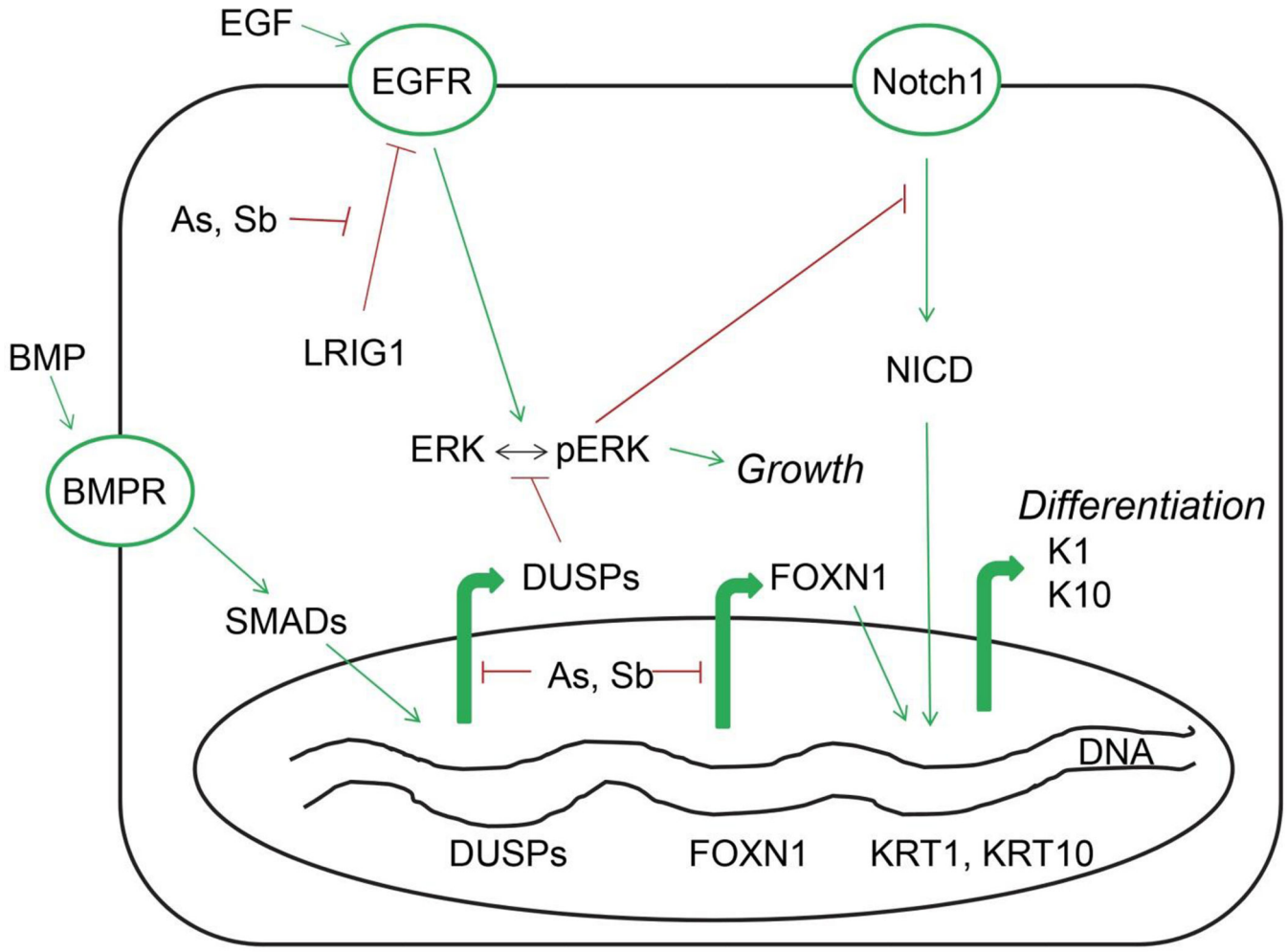

Fig 8.

Signaling pathways involved in keratinocyte growth and differentiation that are perturbed by SbIII and AsIII. Green arrows indicate positive signaling and red lines indicate repression of signaling. The two wavy lines represent nuclear DNA, and thick arrows show RNA transcripts from the indicated genes. Not indicated is the NRF2 pathway.

Table 1
Parallel gene expression responses to SbIII and AsIII

Entries in bold italic were significantly altered in the same directions in protein level

Differentiation markers	**Metabolic enzymes**	**Nrf2 pathway**
Decreased (>3 fold)	***Increased (>1.5 fold)***	***Increased (>2 fold)***
CALML5	ALDOA	***AKR1C3***
CST2	ALDOC	AKR1B1
DSC1	***G6PD***	AKR1B10
FABP5	GAPDH	***FTH***
FLG	ME1	FTL
IVL	PFK	***GCLC***
KRT10	PGM1	GCLM
KRTDAP	PGM3	***HMOX1***
RPTN	PK	ME1
S100A2	TPI1	MT1E
S100A7		MT1X
S100A8		MT2A
S100A9		***NQO1***
S100A12		NQO2
SPRR1A		SRXN1
SPRR1B		TXNRD1
SPRR3		UGT1A6